RSC Advances

PAPER

View Article Online
View Journal | View Issue

Cite this: *RSC Adv.*, 2018, **8**, 41536

Natural phosphate-supported Cu(II), an efficient and recyclable catalyst for the synthesis of xanthene and 1,4-disubstituted-1,2,3-triazole derivatives†

Abbas Amini, *[ab] Azadeh Fallah, *[cd] Chun Cheng[e] and Mahmood Tajbakhsh [f]

Received 6th October 2018
Accepted 28th November 2018

DOI: 10.1039/c8ra08260j

rsc.li/rsc-advances

$Cu(NO_3)_2$ supported on natural phosphate, Cu(II)/NP, was prepared by co-precipitation and applied as a heterogeneous catalyst for synthesizing xanthenes (2–3 h, 85–97%) through Knoevenagel–Michael cascade reaction of aromatic aldehydes with 1,3-cyclic diketones in ethanol under refluxing conditions. It was further used for regioselective synthesis of 1,4-disubstituted-1,2,3-triazoles (1–25 min, 95–99%) *via* a three-component reaction between organic halides, aromatic alkynes and sodium azide in methanol at room temperature. The proposed catalyst, Cu(II)/NP, was characterized using X-ray fluorescence, X-ray diffraction, Fourier-transform infrared spectroscopy, scanning electron microscopy, Brunauer–Emmett–Teller, Barrett–Joyner–Halenda and inductively coupled plasma analyses. Compared to other reports in literature, the reactions took place through a simple co-precipitation, having short reaction time (<3 hours), high reaction yield (>85%), and high recyclability of catalyst (>5 times) without significant decrease in the inherent property and selectivity of catalyst. The proposed protocols provided significant economic and environmental advantages.

Introduction

In recent years, methodological developments have significantly enhanced syntheses of heterocyclic compounds *via* separation/purification processes.[1,2] Recycling catalysts can minimize the consumption of auxiliary substances, concluding in economic and environmental benefits.[3,4]

To significantly enhance the catalytic activity, a support is added to the reaction system; that is, the intimate contact between the supported ions and the support surface can favorably affect the reaction process.[5] Over the past decade, considerable attention has been given to recycling catalysts and heterogeneous metal-based systems,[6] including homogenous metal complexes or noble metals (*e.g.*, Pt, Pd, Au, Ag, Ru, Cu) on inorganic substances (*e.g.*, metal oxides, silica, clay, alumina, carbon) catalysts.[7–9] These exhibit high catalytic activities in a wide range of chemical reactions, for instance, in synthesizing aromatic nitriles from aromatic aldehydes,[10] CO oxidation,[11] carbon dioxide reduction,[12] asymmetric addition of aryl boronic acids to α,β-unsaturated carbonyl compounds,[13] and hydrogenation of CO_2.[14]

Natural phosphate (NP) is a widely available resource in many countries.[15] As it is cheap, nontoxic and non-polluting, major efforts have focused on evaluating its applications in the synthesis of essential compounds.[16] Ma *et al.* reported the adsorption capacity of natural phosphate in immobilizing heavy metals from aqueous solutions.[17,18] Aklil *et al.* examined natural phosphate for the removal of heavy metals from aqueous solution.[18] Natural phosphate was examined to treat soil, waste and wastewater resources contaminated with heavy metals,[19] for the sorption affinity of Pb, Cu and Zn.[20] In these applications, natural phosphate was considered as a support for homogeneous catalysts, due to its chemical and thermal stability, high surface area, and potential sorbents for numerous heavy metals.[21]

Xanthene (1,8-dioxo-octahydroxanthene) is a phenyl with pyran ring fused on either sides along with two other cyclohexanone rings. This compound has biological capability for anti-inflammatory, antibacterial and antiviral activities,[22,23] dye applications,[24] corrosion inhibitory,[25] pH-sensitive fluorescence[26] and laser technologies.[27] For the synthesis of xanthenes, Knoevenagel condensation has been employed followed by the

[a]*Centre for Infrastructure Engineering, Western Sydney University, Kingswood Campus, Bld Z, Locked Bag 1797, Penrith 2751, NSW, Australia. E-mail: a.amini@westernsydney.edu.au; a.amini@ack.edu.kw; Fax: +61-2-9685-9298; Tel: +61-2-404-060-787*

[b]*Department of Mechanical Engineering, Australian College of Kuwait, Mishref, Kuwait*

[c]*Department of Chemistry, Payame Noor University, Tehran, Iran*

[d]*Pharmaceutical Sciences Research Center, Department of Medicinal Chemistry, Mazandaran University of Medical Sciences, Sari, Iran. E-mail: azadehfallah84@gmail.com*

[e]*Department of Materials Science and Engineering, South University of Science and Technology, Shenzhen, China*

[f]*Department of Organic Chemistry, University of Mazandaran, Babolsar, Iran*

† Electronic supplementary information (ESI) available. See DOI: 10.1039/c8ra08260j

Michael addition of carbonyl compounds to 1,3-dicarbonyl compounds along with using a wide range of solid catalysts and inorganic salts. Various catalysts have been reported to promote the synthesis of xanthene, including ICl_3/SiO_2 and $In(CF_3SO_3)_3$,[28] lactic acid,[29] 2,6-pyridinedicarboxylic acid,[30] poly(*N*,*N*′-dibromo-*N*-ethylnaphtyl-2,7-sulfonamide) (PDNES),[31] W-doped ZnO,[32] silica-supported Preyssler nanoparticles,[33] ceric ammonium nitrate-supported HY-zeolite,[34] and Fe_3O_4@SiO_2-imid-$H_3PMo_{12}O_{40}$ nanoparticles.[35] However, these catalysts possess several disadvantages, such as less availability, difficult preparation process, containing toxic organic solvents and harsh reaction conditions (microwave irradiation and high temperature). New catalysts are required to synthesize xanthenes *via* simple, efficient and environmentally friendly processes.

1,2,3-Triazoles belong to an important class of nitrogen-containing heterocyclic compounds with enormous applications in biology, pharmaceutics,[36,37] and medicinal chemistry.[38–41] They are used as corrosion inhibitors,[42] agrochemicals,[43] optical brighteners and dyes.[44] The Huisgen (3 + 2) cycloaddition reaction of azide and alkyne (AAC)[45] was facilitated by Cu(I) catalysts (CuAAC) to afford 1,4-disubstituted-1,2,3-triazoles as a regioselective product.[46,47] CuAAC-reaction was catalyzed by various copper sources, such as Cu(I) salts,[48] *in situ* reduction of Cu(II),[49] oxidation of Cu(0) metal,[50] and Cu(II)/Cu(0) comproportionation.[51] To establish reusable catalysts, Cu(I) AAC catalysts were immobilized onto polymers,[52] zeolite,[53] montmorillonite,[54] silica-supported N-heterocyclic carbine,[55] activated charcoal,[56] alumina,[57] titanium dioxide[58] and CuO nanoparticles.[59,60] Nevertheless, heterogeneous catalysts, immobilized with Cu(I) species, suffer from inherent thermodynamic instability of Cu(I) species, which results in an easy oxidation to Cu(II) and/or disproportionation to Cu(0) and Cu(II)[61] as well as copper nanoparticles.[62] For the AAC reaction, in which Cu(II) species are directly employed, a protocol without deliberate addition of a reducing agent is necessitated.[63]

The present study introduces a new surface modified natural phosphate, Cu(II) supported-natural phosphate, for the synthesis of xanthenes *via* Knoevenagel–Michael cascade reaction of aromatic aldehydes with 1,3-cyclic diketones under refluxing in ethanol (Scheme 1a). This catalyst is further used for the region-selective generation of 1,4-disubstituted-1,2,3-triazoles in a three-component reaction from terminal alkynes, benzyl halides, and NaN_3 in methanol at room temperature (Scheme 1b). With this method, no additional base is needed for the preparation of 1,4-disubstituted-1,2,3-triazoles. The proposed protocols for the synthesis of xanthene and 1,4-disubstituted-1,2,3-triazole present an efficient and robust chemical processes with high yield products at considerable short reaction times. The utilized catalyst in this study (Cu(II)/NP) is recyclable by a simple filtration process, readily available, and easy to prepare with high stability.

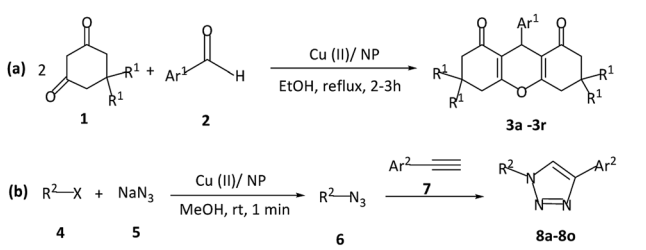

Scheme 1 Preparation of (a) xanthene **3a–3r**, and (b) 1,4-disubstituted-1,2,3-triazole **8a–8o** by Cu(II)/NP, as the heterogeneous catalyst.

Experimental

Reagents and materials

All chemicals were purchased from Merck, Germany, and Sigma Aldrich, USA. The structural data of all synthesized products were compared with the authentic data from literature.

Instrumentation

The chemical compositions of NP and Cu(II)/NP were determined using a PANalytical's XRF spectrometer Venus 200. X-ray powder diffraction analyses were performed at room temperature on a vertical Philips PW1050/25 goniometer mounted with Bragg–Brentano configuration (θ, 2θ) using Ni-filtered Cu-K_α radiation ($\lambda = 1.54$ Å) and facilitated with the PANalytical X'Pert High Score Plus software. The surface imaging was performed using a scanning electron microscope (SEM) EM-3200. Surface areas were characterized at 77 K using a Coulter SA 31000 instrument through an automated gas volumetric method with nitrogen as the adsorbate. Fourier Transform Infrared (FT-IR) spectra were recorded on a Bruker Tensor 27 spectrometer, using KBr pellets for solids. ^{1}H and ^{13}C Nuclear Magnetic Resonance (NMR) spectra were recorded using a Bruker Advance DRX spectrometer at 400 MHz in DMSO-d_6 and $CDCl_3$ with tetra-methyl-silane as the internal reference.

Preparation of catalyst

Different metal salts, including $NaNO_3$, NaCl, KF, $Cu(NO_3)_2$, $Ni(NO_3)_2$, $CuCl_2$, $CoCl_2$, were doped on NP. They were prepared by adding 5 g NP to the aqueous metal salts solution (50 mL, 0.4 M). The mixture stirred at room temperature for 1 hour, then, the water content was evaporated at vacuum pressure. The suspended solid was calcined in air at three different temperatures of 160 °C for NaCl, 150 °C for KF, $NaNO_3$, $Cu(NO_3)_2$, $Ni(NO_3)_2$, $CuCl_2$, $CoCl_2$ and 105 °C for $Cu(NO_3)_2$.[64]

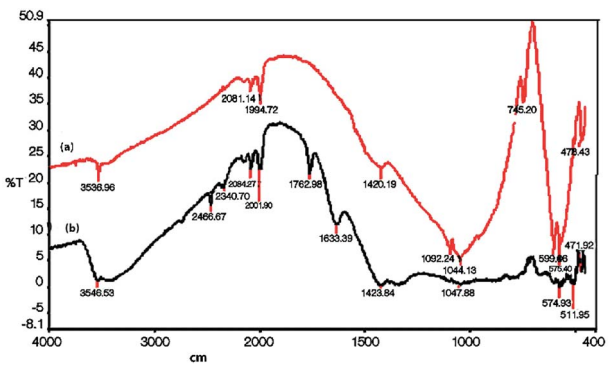

Fig. 1 FT-IR spectrum (a) NP, (b) Cu(II)/NP.

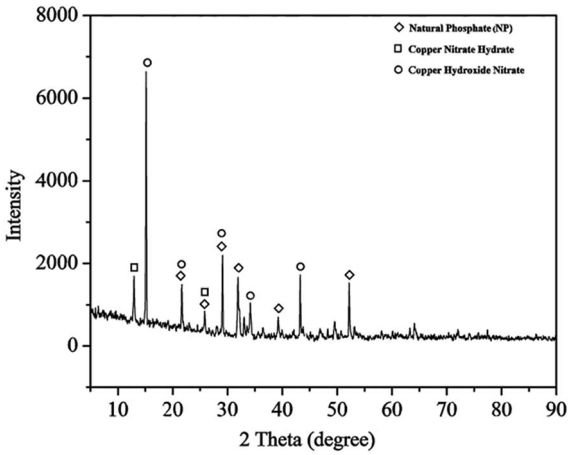

Fig. 2 X-ray diffraction of Cu(II)/NP.

Preparation and characterization of Cu(II)/NP catalyst

NP was collected from ore resources in Yazd (Iran). NP was refluxed in water for 4 hours, then, filtered and washed with water, dried at 80 °C overnight and calcined at 900 °C for another 2.5 hours. The obtained solid was washed again and recalcined at 900 °C for 30 minutes. To obtain Cu(II)/NP, NP (5 g) was added to an aqueous $Cu(NO_3)_2 \cdot 3H_2O$ solution (50 mL, 0.4 M). The mixture was stirred at room temperature for 30 minutes, then, evaporated in vacuum. The final solid was calcined under air at 105 °C for 2 hours.

Synthesis of xanthenes

To a solution of aromatic aldehyde (1 mmol) and diketone (2 mmol) in ethanol (3 mL), Cu(II)/NP catalyst (0.2 g) was added and refluxed 2–3 hours to result xanthene **3**, while the reaction progress was characterized by TLC (silica gel, hexane : EtOAc, 7 : 3). After the completion of reaction, the mixture was filtered and washed with hot ethanol (boiling). Evaporation of the ethanoic filtrate provided xanthene **3** (Scheme 1(a)), the melting point of the final product was characterized through FT-IR, ^{1}H and ^{13}C NMR spectra. Selected spectral data of some obtained xanthenes are as follow:

9-(4-Bromo-phenyl)-3,3,6,6-tetramethyl-3,4,5,6,7,9-hexahydro-2*H*-xanthene-1,8-dione (3b). White solid; mp = 240–242 °C,[65] IR (KBr, cm^{-1}): υ = 2952.5, 2875.3, 1658.5, 1361.5, 1197.6, 1004.7. ^{1}H NMR (400 MHz, $CDCl_3$): δ = 7.35 (d, 2H, J = 6.4 Hz, H–Ar), 7.20 (d, 2H, J = 8.8 Hz, H–Ar), 4.71 (s, 1H, H_9), 2.47 (t, 4H, $2CH_2$), 2.21 (q, 4H, $2CH_2$), 1.11 (s, 6H, 2Me), 1.00 (s, 6H, 2Me). ^{13}C NMR (400 MHz, DMSO-d_6): δ (ppm) = 196.3, 162.4, 143.2, 131.1, 130.2, 120.2, 115.2, 50.7, 40.8, 32.2, 31.6, 29.3, 27.3. Calcd for $C_{23}H_{25}BrO_3$: C, 64.34; H, 5.87; Br, 18.16. Found: C, 64.32, H, 5.85; Br, 18.59.

4-(3,3,6,6-Tetramethyl-1,8-dioxo-2,3,4,5,6,7,8,9-octahydro-1*H*-xanthen-9-yl) benzonitrile (3c). White solid; mp = 222–224 °C,[66] IR (KBr, cm^{-1}): υ = 2952.5, 2875.3, 2260.5, 1660.4, 1471.4, 1361.5, 1197.6, 1151.3, 1004.7, 844.7. ^{1}H NMR (400 MHz, $CDCl_3$): 7.53 (d, 2H, J = 8.0 Hz, H–Ar), 7.43 (d, 2H, J = 8.0 Hz, H–Ar), 4.78 (s, 1H, H-9), 2.50 (brs, 4H, $2CH_2$), 2.25 (d, 2H, J = 16 Hz, CH_2), δ (ppm) = 2.15 (d, 2H, J = 16 Hz, CH_2), 1.13 (s, 6H, 2Me), 1.00 (s, 6H, 2Me). ^{13}C NMR (400 MHz, $CDCl_3$): δ (ppm) = 196.4, 162.4, 142.7, 132.0, 129.8, 128.2, 115.2, 50.7, 40.8, 32.2, 31.5, 29.33, 27.3. Anal. calcd for $C_{24}H_{25}NO_3$: C, 76.77; H, 6.71; N, 3.73. Found: C, 76.71, H, 6.69; N, 3.71.

Synthesis of 1,4-disubstituted-1,2,3-triazoles

Cu(II)/NP catalyst (0.06 g) was added to a stirred suspension of NaN_3 (78 mg, 1.2 mmol), alkyl halide (1.0 mmol) and methanol (2 mL). The procedure was followed by slow drop-wise addition of a solution of terminal alkyne (1.0 mmol) and methanol (2 mL). The mixture was stirred at room temperature, after the completion of reaction, it was characterized by TLC (silica gel, hexane : EtOAc, 7 : 3). The mixture was filtered and washed with methanol. All the products were carefully isolated from methanol or a mixture of ethanol/water (1 : 3, v/v) through recrystallization. The spectral data (^{1}H, ^{13}C NMR) of the obtained products were evaluated with the spectra of authentic samples

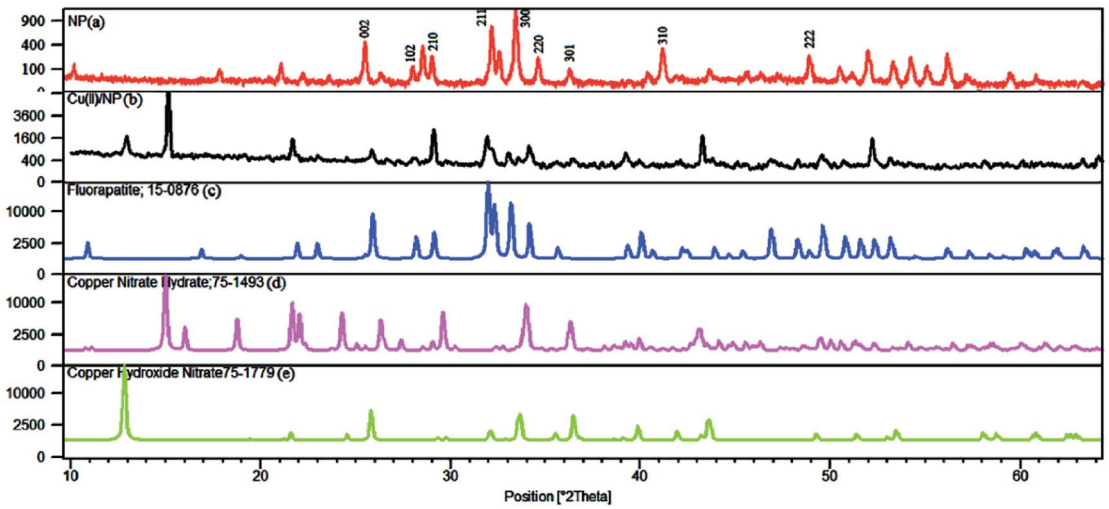

Fig. 3 X-ray diffraction of (a) NP, (b) Cu(II)/NP, (c) fluorapatite, (d) copper nitrate hydrate, (e) copper hydroxide nitrate.

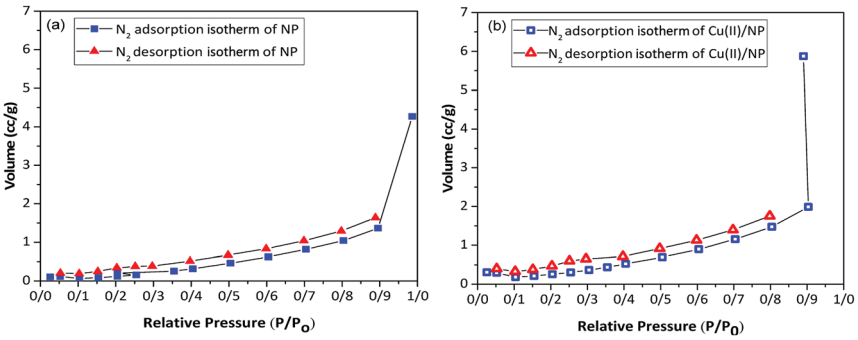

Fig. 4 N_2 adsorption–desorption isotherm (BET) of (a) NP, and (b) Cu(II)/NP.

reported in literature. Selected spectral data of some obtained 1,4-disubstituted-1,2,3-triazoles are presented below:

1-Benzyl-4-phenyl-1*H*-1,2,3-triazole (8a). Mp = 133–134 °C,[67] ^{1}H NMR (400 MHz, $CDCl_3$): δ (ppm) = 7.82 (d, J = 7.2 Hz, 2H), 7.70 (s, 1H), 7.44–7.32 (m, 8H), 5.60 (s, 2H). ^{13}C NMR (100 MHz, $CDCl_3$): δ (ppm) = 148.15, 134.67, 130.52, 129.08, 128.74, 128.70, 128.09, 127.99, 125.65, 119.48, 54.15.

1-(4-Bromobenzyl)-4-phenyl-1*H*-1,2,3-triazole (8b). Mp = 156–158 °C,[67] ^{1}H NMR (400 MHz, $CDCl_3$): δ (ppm) = 7.83 (d, J = 7.2 Hz, 2H), 7.73 (s, 1H), 7.53 (d, J = 8.4 Hz, 2H), 7.43 (t, J = 7.4 Hz, 2H), 7.34 (t, J = 7.4 Hz, 1H), 7.20 (d, J = 8.4 Hz, 2H), 5.54 (s, 2H). ^{13}C NMR (100 MHz, $CDCl_3$): δ (ppm) = 53.59, 118.75, 122.97, 125.69, 128.29, 128.86, 129.67, 130.43, 147.04, 133.71, 132.34.

Results and discussion

Characterization of Cu(II)/NP catalyst

The FT-IR spectrum of NPs shows strong peaks at: 1092, 1044, 600, 576 and 473 cm^{-1} which can be referred to the vibrational modes of P–O, P–O–P bands in PO_4^{3-} groups of the apatite structure (Fig. 1a).[68] In the spectrum of Cu(II)/NPs, these bands are weakened or disappeared (Fig. 1b). The FT-IR characterization of Cu(II)/NP shows strong bands with the maximums at ~1633 and 1423 cm^{-1}, which are associated to N=O, O–NO–O bands and nitrate groups of $Cu(NO_3)_2 \cdot 3H_2O$. The strong absorption peak at 3480 cm^{-1} attributes to H_2O absorbed either in the samples or in the KBr pellet. These spectra show that the decomposition of nitrate does not happen at the temperature of calcination (105 °C).[15]

Table 1 Surface properties of NP and Cu(II)/NP

	Specific surface area [m^2 g^{-1}]		Specific pore volume [cm^3 g^{-1}]		Pore diameter [nm]	
Sample	S_{BET}	S_{BJH}	$V_{tot\ BET}$	V_{BJH}	$D_{average}$	D_{BJH}
NP	2.081	1.948	0.00662	0.00722	12.73	3.675
Cu(II)/NP	1.849	2.513	0.00912	0.00972	19.70	3.089

The X-ray diffraction (XRD) patterns of Cu(II)/NP in Fig. 2 show sharp and distinct peaks which confirm a high degree of crystallinity.[69] The structure of NP is shown to be modified by the solid phase reaction with copper nitrate ($Cu(NO_3)_2$). The XRD peaks fit with standard patterns of fluorapatite JCPDS 15-876 (Fig. 3c), and some other new crystalline phases, including copper nitrate hydrate, $Cu(NO_3)_2(H_2O)_{2.5}$, JCPDS 75-1493 (Fig. 3d), and copper hydroxide nitrate, $Cu_2(OH)_3(NO_3)$, JCPDS 75-1779 (Fig. 3e). Compared to NPs, the intensity of typical diffraction peaks of Cu(II)/NP significantly differs, which indicates disordering the crystalline structure of Cu(II)/NP. No detection of $Cu(NO_3)_2$ phase on the doped materials implies that $Cu(NO_3)_2$ is highly dispersed in NP.[70] CaO phase (2θ = 32.2, 37.5 and 54.0°) has no peaks, which verifies no solid phase reaction between the supported copper nitrate and the calcium phosphate of NP during the copper nitrate decomposition process.[12,70] From the XRD curves of Cu(II)/NP (Fig. 2), it is concluded that copper phosphate or any other types of mixed calcium copper phosphate does not combine with the NP

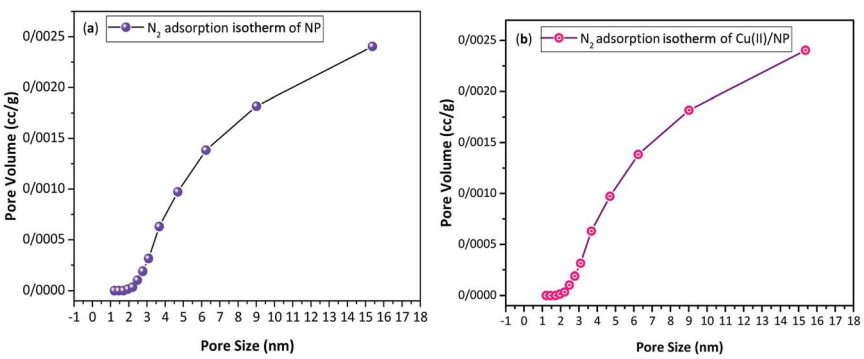

Fig. 5 Pore size distribution curve (BJH) of: (a) NP, and (b) Cu(II)/NP.

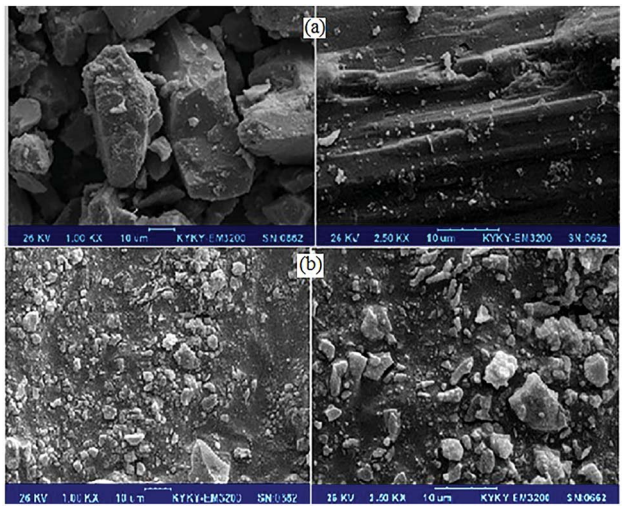

Fig. 6 SEM images of: (a) NP, and (b) Cu(II)/NP.

crystalline framework. The remarkable fact is that the main modifications in the pattern are produced in the range of $2\theta =$ 12–15°, with new lines at 12.92° and 15.13° together with an increase in the intensity of other lines (Fig. 2). The intense lines related to NP are weakened against fluorapatite (see Fig. 3a–c); the lack of intense bands may account for the formation of very small crystals, partially amorphous materials or mixed phosphates with different stoichiometry.[16]

The porosity of Cu(II)/NP is investigated *via* Brunauer–Emmett–Teller (BET) (Fig. 4) and Barrett–Joyner–Halenda (BJH) (Fig. 5) methods using N_2 adsorption–desorption isotherms. The type IV isotherm of Cu(II)/NP possesses a hysteresis loop and typical property of mesoporous materials (2–50 nm), such as high surface areas (>1000 m^2 g^{-1}), large internal pore volumes and unique ordered porous structures, similar to NP, but at a higher relative pressure of N_2 gas. The surface area of Cu(II)/NP is higher compared to other mesoporous NPs with no Cu particles (Fig. 4). The N_2 adsorption–desorption isotherms of NP and Cu(II)/NP are measured by BET and BJH methods, where

Table 2 Synthesizing xanthene **3a** using various solid catalysts[a]

Entry	Catalyst	Calcination temperature (°C)	Time (h)	Isolated yield **3a** (%)
1	NP[78]	900	6.5	90
Present study				
2	$NaNO_3$/NP	150	6.5	15
3	NaCl/NP	160	5	70
4	KF/NP	150	5	10
5	$Cu(NO_3)_2$/NP	500	48	15
6	$Cu(NO_3)_2$/NP	150	6	50
7	$Cu(NO_3)_2$/NP	105	2	98
8	$Ni(NO_3)_2$/NP	150	5	25
9	$CuCl_2$/NP	150	3.5	98
10	$CoCl_2$/NP	150	6.5	20

[a] Reaction conditions: 4-chlorobenzaldehyde (1 mmol), dimedone (2 mmol), catalyst (0.2 g) in refluxing EtOH (3–5 mL).

Table 3 Effect of copper nitrate concentration, supported on NP, and the catalyst loading for the synthesis of xanthene **3a** [a]

Entry	Catalyst	Catalyst loading (g)	Time (h)	Yield **3a** (%)
1	$Cu(NO_3)_2$(0.2 M)/NP	0.2	7	70
2	$Cu(NO_3)_2$(0.2 M)/NP	0.5	7	90
3	$Cu(NO_3)_2$(0.3 M)/NP	0.1	4	90
4	$Cu(NO_3)_2$(0.3 M)/NP	0.2	3	89
5	$Cu(NO_3)_2$(0.4 M)/NP	0.1	4	92
6	$Cu(NO_3)_2$(0.4 M)/NP	0.15	3	95
7	$Cu(NO_3)_2$(0.4 M)/NP	0.2	2	98
8	$Cu(NO_3)_2$	0.064	4	50

[a] Reaction conditions: dimedone (2 mmol), 4-chlorobenzaldehyde (1 mmol), catalyst in refluxing EtOH (3–5 mL).

the special surface area (S), the total pore volume ($V_{tot\ BET}$), micro pore volume (V_{BJH}), and the average pore diameter ($D_{average}$) are calculated using the adsorption data. The special surface area (S_{BET}) of NP and Cu(II)/NP is calculated through BET method and the surface area of meso-pore S_{BJH}, and the meso-pore volume V_{BJH} of NP and Cu(II)/NP are calculated using BJH method (Table 1). According to the classification standard of International Union of Pure and Applied Chemistry (IUPAC), the characteristics of NP and Cu(II)/NP as mesoporous solids display a type IV isotherm with H3 hysteresis loop.[71,72] According to BET and BJH results, the shape of Cu(II)/NP was similar to NPs, and the porosity of Cu(II)/NP did not change during the stabilization of Cu(II) on the surface of NP. These results introduced permanent porosity of the Cu(II)/NP surface. From Table 1, according to the BET calculation, the specific surface area decreased from 2.081 m^2 g^{-1} for NP to 1.849 m^2 g^{-1} for Cu(II)/NP. These observations verified no clogging of pores with copper species.[73] The specific pore volume increased after supporting NP with copper nitrate. After loading Cu(II), larger pores generated; as a result, the average pore diameter increased from 12.73 to 19.70 nm.[74] The BJH curves of nitrogen adsorption displayed a decline in pore diameter from 3.67 to 3.08 nm, which was originated from introducing copper species

Table 4 Effect of various solvents on the reaction time and yield of 1,4-disubstituted-1,2,3-triazole **8a** upon using Cu(II)/NP

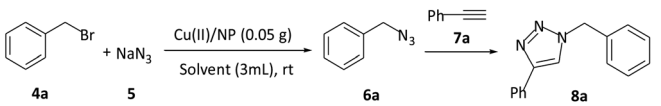

Entry	Solvent	Time (min)	Isolated yield **8a** (%)
1	H_2O	60	10
2	EtOH	60	90
3	**MeOH**	**15**	**95**
4	CH_2Cl_2	120	25
5	CH_3CN	90	20
6	CH_3OAc	120	5
7	THF	90	80
8	1,4-Dioxane	120	5

Table 5 Effect of Cu(II)/NP loading on the synthesis of 1,4-disubstituted-1,2,3-triazole **8a**[a]

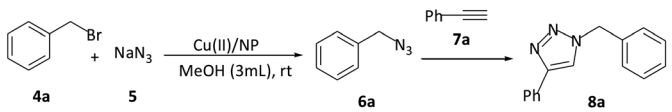

4a 5 6a 8a

Entry	Cu(II)/NP (g)	Time (min)	Isolated yield **8a** (%)
1	0.01	120	10
2	0.02	90	62
3	0.03	60	73
4	0.04	45	87
5	0.05	15	95
6	0.06[a]	1	99

[a] Cu content is 0.026 g: 6.7% mol.

complex to the interior side of some pores in NP.[75] High surface area and large pore size of Cu(II)/NP favoured a high dispersion of active elements, and made the large amounts of the reactive molecules to be easily accessible.[76]

Surface structure of Cu(II)/NP was investigated by SEM method in order to visualise the textural modifications after adding copper nitrate to natural phosphate (Fig. 6). Compared to NP (Fig. 6a), Cu(II)/NP (Fig. 6b) had a rougher surface with more distorted areas, along with uniform spherical particles. In fact, the addition of copper nitrate increased the size of catalyst particles in Cu(II)/NP.[15,72,77]

Coupling reaction-based synthesis of xanthenes

Authors have introduced NP as a catalyst for synthesizing xanthene derivatives through the reaction of 4-chlorobenzaldehyde (1 mmol) with dimedone (2 mmol) in refluxing ethanol.[78] To afford xanthene **3** with a high yield, relatively high weight of NP catalyst (1.5 g) and long reaction time are required (Table 1, no. 1). Here, to increase the NP activity, it is doped with different metal salts (*i.e.*, sodium nitrate, $NaNO_3$; sodium chloride, NaCl; potassium fluoride, KF; nickel nitrate, $Ni(NO_3)_2$; copper nitrate, $Cu(NO_3)_2$; cobalt chloride, $CoCl_2$; and copper chloride, $CuCl_2$) (Table 2). The results show that copper salts are the best candidates to synthesize xanthene **3a** (Table 2, entries 7 and 9). Table 2 (entries 5–7) represents the results of calcination temperatures for preparing $Cu(NO_3)_2$/NP. The treatment of $Cu(NO_3)_2$/NP at 150 and 500 °C led to catalysts with poor or no catalytic activities (Table 2, entries 5 and 6). This is due to thermal decomposition of nitrate groups of $Cu(NO_3)_2$/NP at temperatures over 200 °C as well as the formation of the copper oxide (CuO).[77] The decomposition of d-metal nitrates hydrates proceeded with slow pace that rarely led to anhydrous salts. Usually the dehydration process is not complete and the beginning of nitrate (V) groups decomposition occurs simultaneously with the evolution of water hydration.[79] The following molecular and fragmentation ions of H_2O^+, NO^+, N_2O^+, NO_2^+ can be formed during the decomposition of nitrates. These ionic products from the decomposition of copper nitrate concluded in the formation of copper hydroxide nitrate, $Cu_2(OH)_3(NO_3)$ and copper nitrate hydrate, $Cu(NO_3)_2(H_2O)_{2.5}$[77] which in our study were confirmed by XRD analysis (Fig. 2). At the lower calcination temperature, *e.g.*, 105 °C, a high yield (98%) of **3a** was created in a short reaction time (Table 2, entry 7). In fact, the initial state of Cu on the support was $Cu(NO_3)_2 \cdot 3H_2O$ and the final state of Cu on the support was copper nitrate hydrate, $Cu(NO_3)_2(H_2O)_{2.5}$, copper hydroxide nitrate and $Cu_2(OH)_3(NO_3)$, supported on the surface of NP. The decomposition of nitrate groups proceeded at the same temperature range as dehydration did.

The treatment at 500 °C resulted in a very low yield 15% of **3a** after a long period of reaction time 48 hours (Table 2, entry 5). The decomposition of Cu(II) species to copper oxide was confirmed by the decreased weight of catalyst, its black color and reported results from other researchers.[77] The non-catalytic activity of $Cu(NO_3)_2$/NP [calcinated at 500 °C] might be due to the formation of copper oxide on NP and its non-porous surface morphology of copper oxide.[80] As previously reported,[78] this reaction under the same condition is carried out by using NP as catalyst, which provides 90% high yield of **3a** in a little long reaction time 6.5 hours (Table 2, entry 1). When NP is modified by $Cu(NO_3)_2$, the reaction time decreases to 2 hours and the yield of the products increases to 98% (Table 2, entry 5). In short, compared to NP, $Cu(NO_3)_2$/NP calcined at 105 °C produces xanthenes with much higher yields at shorter reaction times.

In order to determine the best ratio of $Cu(NO_3)_2$/NP, supported copper catalyst was prepared by impregnating NP with different concentrations of $Cu(NO_3)_2 \cdot 3H_2O$ aqueous solution (0.1, 0.2, 0.3, and 0.4 M). These supported copper catalysts were prepared according to the procedures introduced in Sections 2.3 and 2.4. Their catalytic effect on the yield and time of the reaction of 4-chlorobenzaldehyde with dimedone for the synthesis of xanthene **3a** as model reaction were investigated (Table 3). As shown in Table 3, the best result was obtained by $Cu(NO_3)_2$/NP, prepared with 0.4 molar concentration of $Cu(NO_3)_2 \cdot 3H_2O$ aqueous solution; we name it Cu(II)/NP (Table 3, entry 7). To determine the effect of support in the reaction, the catalytic effect of sole $Cu(NO_3)_2$ was investigated in the model reaction. The unsupported copper catalyst was prepared *via* calcination of $Cu(NO_3)_2 \cdot 3H_2O$ at 105 °C for 2 hours. In order to determine the role of NP in the catalytic activity of Cu(II)/NP, the amount of copper nitrate existed in 0.2 g Cu(II)/NP was calculated as 0.064 g. So, 0.064 g of $Cu(NO_3)_2$ was used as catalyst in the model reaction; it afforded **3a** only with 50% of yield after 4 hours (Table 3, entry 8). The result show that, in contrast with NP, the sole modified $Cu(NO_3)_2$ cannot positively affect the reaction time and yield of **3a**.

Click-reaction-base synthesis of 1,4-disubstituted-1,2,3-triazoles

The catalytic activity of Cu(II)/NP was studied in the 1,3-dipolar cycloaddition reactions using benzyl bromide (**4a**), sodium azide (**5**, 1.1 mmol) and phenyl acetylene (**7a**) as model

Table 6 Synthesis of 1,4-disubstituted-1,2,3-triazole derivatives by using Cu(II)/NP as catalyst

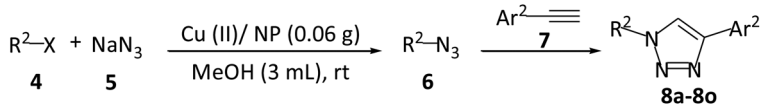

Entry	X	R^2	Ar^2	Product **8**	Time (min)	Isolated yield **8** (%)
1	Br	$C_6H_5CH_2$	C_6H_5	**8a**	1	99
2	Br	4-Br$C_6H_4CH_2$	C_6H_5	**8b**	5	99
3	Br	4-$NO_2C_6H_4CH_2$	C_6H_5	**8c**	10	97
4	Cl	3,5-$Cl_2C_6H_3CH_2$	C_6H_5	**8d**	10	98
5	Cl	$C_6H_5CH_2$	C_6H_5	**8e**	15	98
6	Br	2-Cl$C_6H_4CH_2$	C_6H_5O	**8f**	20	96
7	Cl	$C_6H_5CH_2$	C_6H_5O	**8g**	20	96
8	Br	4-Br$C_6H_4CH_2$	C_6H_5O	**8h**	20	95
9	Br	4-$NO_2C_6H_4CH_2$	C_6H_5O	**8i**	25	95
10	Cl	3,5-$Cl_2C_6H_3CH_2$	C_6H_5O	**8j**	25	96
11	Cl	2-Cl$C_6H_4CH_2$	C_6H_5O	**8k**	20	96
12	Br	$C_6H_5CH_2$	4-Br-C_6H_4O	**8l**	15	97
13	Br	$C_6H_5CH_2$	3,5-Cl_2-C_6H_3O	**8m**	20	95
14	Br	4-$NO_2C_6H_4CH_2$	4-Br-C_6H_4O	**8n**	10	96
15	Br	4-$NO_2C_6H_4CH_2$	3,5-Cl_2-C_6H_3O	**8o**	15	94

substrates under various conditions. This three-component reaction proceeded *via in situ* formation of benzyl azide from benzyl bromide and sodium azide. Benzyl azide underwent the 1,3-dipolar cycloaddition reaction with phenyl acetylene (**7a**) to afford 1-benzyl-4-phenyl-1*H*-1,2,3-triazole (**8a**). This model reaction was carried out in different solvents with Cu(II)/NP (0.05 g) at room temperature (Table 4). Among the used solvents, the best result was earned from using methanol with 95% yield of the desired product **8a** after 15 minutes (Table 4, entry 3). The model reaction with EtOH synthesized the product **8a** with an excellent yield (90%) after a longer reaction time (60 minutes) (Table 4, entry 2).

The catalyst loading of the model reaction was investigated in the synthesis of 1,4-disubstituted-1,2,3-triazole **8a** (Table 5). 0.06 g of Cu(II)/NP (with 6.7 mol% Cu content) afforded the best yields with ~100% isolated yield of 1,4-disubstituted-1,2,3-triazole **8a** after 1 minute (Table 5, entry 6), whereas $Cu(NO_3)_2 \cdot 3H_2O$ (0.026 g, 6.7 mol%) afforded 70% yield after 2 hours.

By implementing the optimized conditions (Cu(II)/NP 0.06 g, methanol (3 mL), room temperature), various aryl halides and sodium azide were reacted with various terminal acetylenes for the synthesis of 1,4-disubstituted-1,2,3-triazole **8** (Table 6). The desired 1,4-disubstituted-1,2,3-triazole derivatives were synthesized and characterized by checking reported melting points of related products in the literatures and spectroscopic methods. As shown in Table 6, corresponding products were obtained with excellent yields in short reaction times at room temperature.

A proper supported catalyst should not leach to the reaction mixture. The recyclability of the supported catalyst is another important characteristic which should not suffer from mechanical degradation.[81] As such, Cu(II)/NP did not suffer from extensive mechanical degradation after running the tests. Here, the separated Cu(II)/NP from the reaction was dried at room temperature and calcined at 105 °C for half an hour for its recovery and reuse. The catalyst leaching in the reaction media was evaluated by measuring the copper content in recycled Cu(II)/NP, by means of Inductively Coupled Plasma (ICP) analysis. From the ICP analysis, the copper contents of fresh catalyst and 5th run reused catalyst were 20.3 and 16.4 w/w%, respectively. The difference of copper contents between fresh and reused catalyst (5th run) was only 4 w/w%.[20,82] After the calculation, 0.056 g of Cu(II) existed in 5th recycled Cu(II)/NP rather than 0.064 g of Cu(II) in fresh Cu(II)/NP, so 0.008 g of Cu(II) was removed (Table 3, entry 8). This indicated very low leaching amount of copper catalyst into the reaction mixture. So, Cu(II)/NP can be reused up to 5 runs without any significant decline in the yield during the synthesis of xanthene **3a** (Fig. 7), and 6 runs during the synthesis of 1,4-disubstituted-1,2,3-triazole **8a** (Fig. 8).

The surface of Cu(II)/NP possesses multiple catalytic active sites.[83] The excellent catalytic efficiency was mainly corresponded to the surface cooperation between the Lewis basic sites of NP (oxygen in phosphate PO_4 and calcium oxide

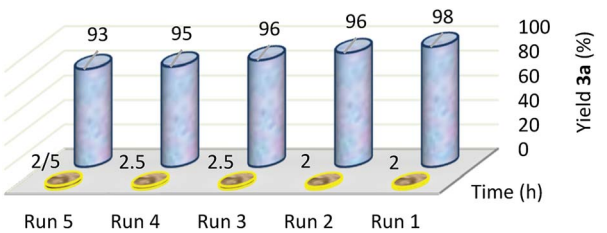

Fig. 7 Recyclability of Cu(II)/NP in coupling reaction for the synthesis of xanthene **3a**. Reaction conditions: 4-chlorobenzaldehyde (1 mmol), dimedone (2 mmol), Cu(II)/NP (0.2 g) in refluxing EtOH (3–5 mL).

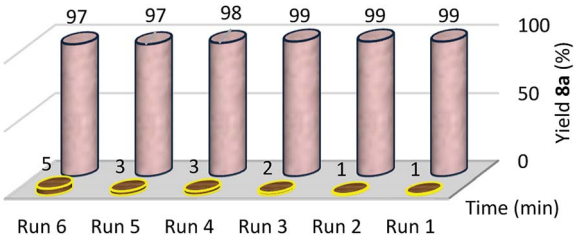

Fig. 8 Recyclability of Cu(II)/NP in click reaction for the synthesis of 1,4-disubstituted-1,2,3-triazole **8a**. Reaction conditions: benzyl bromide (1 mmol), NaN_3 (1.1 mmol), phenyl acetylene (1 mmol) and Cu(II)/NP (0.06 g) in MeOH (3 mL) at room temperature.

CaO)[84] and the Lewis acidic site of adjacent Cu^{+}/Cu^{++} species (copper ion Cu^{2+} coordinated with the basic sites of NP surface).[84,85] The basic sites on NP held the key role in the abstraction of protons from the methylene in 1,3-diketones.[84] Further, the carbonyl group of aldehyde interacted with the acidic sites (Cu^{2+}) of Cu(II)/NP, thereby, activated the carbonyl carbon for the nucleophilic attack. So, the Knoevenagel–Michael cascade reactions accelerated the Knoevenagel–Michael cascade reactions for the synthesis of xanthenes[86] (Scheme 2). According to previous reports,[83] a stepwise mechanism can be proposed for synthesizing 1,4-disubstituted-1,2,3-triazoles (Scheme 3). In stage 1, benzyl azide was formed *in situ* beside the terminal hydrogen of alkyne. It deprotonated in the basic medium of NP, while Cu(I) acetylide formed through the π-alkyne copper complex intermediate I. This π-coordination of alkyne with copper was activated to form σ-acetylide (stage 2). Then, the azide was activated by the coordination with copper to form intermediate II (stage 3). The coordination phenomena were synergistic for both reactive partners in intermediates I and II. Coordination of azide revealed the β-nucleophilic which resulted in vinylidene-like properties of acetylide. So, the azide's terminus became even more electrophilic and a strained copper triazolide B was formed (stage 4). Protonation of B, followed by the dissociation of product 8, completed the reaction, transferred the dehydrogenation of basic sites on NP (stage 5), and regenerated the catalyst Cu(II)/NP.

To illustrate the efficiency of present protocols for the synthesis of xanthene, our results are compared with the existing results in literature (Table 7). As shown in Table 7, the synthesis of xanthene with Fe^{+3}-montmorillonite, alumina-sulfuric acid and SBSSA, the preparation of catalyst needs more time (at least 48 hours). It also includes several steps and working with hazardous and expensive materials (Table 7, entries 1, 2 and 5). By using other catalysts, *e.g.*, SBSAN, ICl_3/SiO_2, $In(CF_3SO_3)_3$, PANI-PTSA and Nano $ZnAl_2O_4$, the reactions are completed in a little shorter period of time than our process, however, they suffer from their difficult, multi-step and costly routs as well as extra material preparation (Table 7, entries 3–8). Using LUS-Pr-SO_3H is accomplished under harsh reaction conditions, in a longer period, and multi-step preparation process which requires more devices (Table 7, entry 9). The reaction by [cmmim][BF_4] as the catalyst takes place under microwave condition and suffers from the harsh reaction

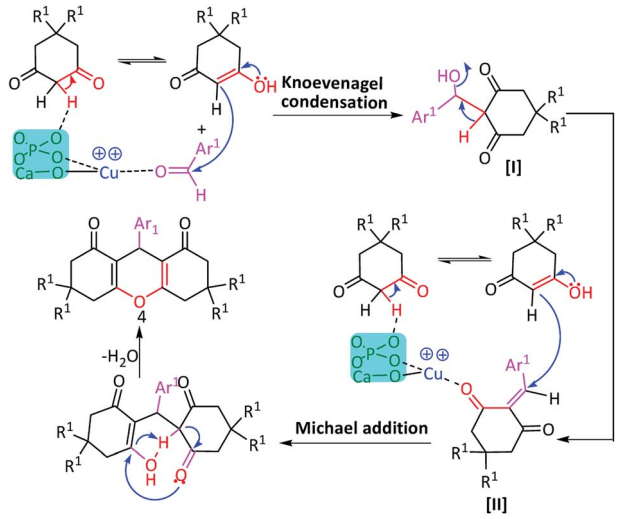

Scheme 2 Plausible mechanism for synthesis of xanthene while using Cu(II)/NP catalyst.

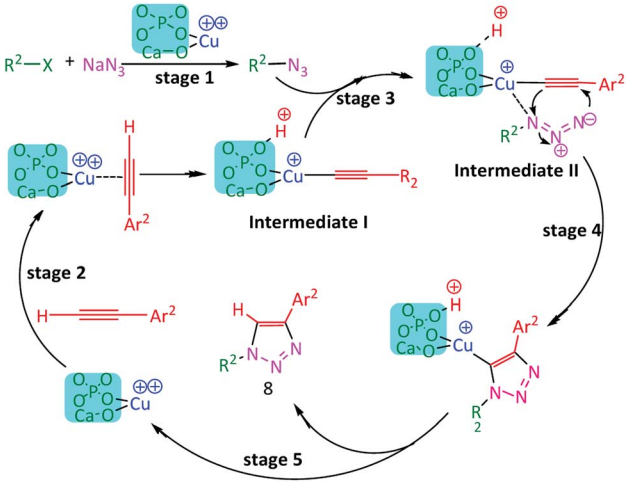

Scheme 3 Plausible mechanism for one-pot CuAAC protocol synthesis of 1,4-disubstituted-1,2,3-triazole while using Cu(II)/NP catalyst.

conditions (Table 7, entry 10). The reaction by NP needs a high amount of NP at a long reaction time (Table 7, entry 11).

To illustrate the efficiency of present protocols for the synthesis of 1,4-disubstituted-1,2,3-triazole derivatives, the results are compared with the existing results in literature (Table 8). Different catalysts are used for the synthesis of 1,4-disubstituted-1,2,3-triazole derivatives which suffer from several disadvantages. For example, by using Cu/Al_2O_3 and Cu/SiO_2 as catalysts, the reactions are performed under harsh conditions, such as ball-milling and MW irradiation (Table 8, entries 2 and 4). The preparation process of some other catalysts, *i.e.*, Cu(II)-PBS–HPMO and SiO_2–NHC–Cu(I), is multistep at a long period of time under 100 °C and 80 °C, respectively (Table 8, entries 5 and 9). CuNP/C as the catalyst can result in a desired product with 99% yield but it needs 70 °C temperature and

Table 7 Comparison of the reaction conditions and results for the synthesis of xanthene **3a** [a]

Entry	Catalyst	Condition	Time	Yield **3a** (%)	Ref.
1	Fe^{+3}-montmorillonite (15 wt%)	100 °C/EtOH	6 h	97	87
2	Alumina-sulfuric acid (200 mg)	Reflux/EtOH	4 h	83	88
3	SBSAN[b] (0.5 g)	50 °C/solvent-free	2 h	95	89
4	PANI-PTSA[c] (25 wt%)	Reflux/H_2O	6 h	75	90
5	SBSSA[d] (0.1 g)	Reflux/EtOH	10 h	98	91
6	Nano $ZnAl_2O_4$ (90 mg)	Reflux/EtOH	15 min	88–98	92
7	ICl_3/SiO_2 (5 mol%)	75 °C/solvent free	1 h	90	28
8	$In(CF_3SO_3)_3$ (2 mol%)	100 °C/solvent free	1 h	95	28
9	LUS-Pr-SO_3H[e] (0.02 g)	140 °C/solvent free	15 min	90	93
10	[cmmim][BF_4] (0.2 g)	80 °C/solvent free, MW	2 h	94	94
11	NP (1.5 g)	Reflux/EtOH	6.5 h	90	78
12	Cu(II)/NP (0.2 g)	Reflux/EtOH	2 h	98	This study

[a] Reaction conditions: dimedone (2 mmol), 4-chlorobenzaldehyde (1 mmol), catalyst. [b] Silica boron-sulfuric acid nano particles (SBSAN). [c] Nano ferrite-glutathione-copper (PANI-PTSA). [d] Silica bonded S-sulfonic acid (SBSSA). [e] Propyl sulfonic acid functionalized LUS-1 (Laval University silica) (LUS-Pr-SO_3H).

Table 8 Comparison of the reaction conditions for the synthesis of 1,4-disubstituted-1,2,3-triazole **8a**[a]

Entry	Catalyst	Condition	Time	Yield **8a** (%)	Ref.
1	2-Pyrrole carbaldiminato–Cu(II) complex (0.005 mmol)	Rt/H_2O	13 h	97	63
2	Cu/Al_2O_3 (10 mol%)	Ball-milling, rt/neat	1 h	92	95
3	Cu(I)-zeolite (10 mol%)	20 °C/MeOH	15 h	80	96
4	Cu/SiO_2 (20 mol%)	MW, 70 °C/H_2O	10 min	92	97
5	Cu(II)-PBS[b]–HPMO (10 mg)	100 °C/H_2O	3.5 h	96	98
6	CuNP/C[c] (0.5 mol%)	70 °C/H_2O	6 h	99	99
7	CuNP[d] (0.025 mmol)	rt/MeOH	8 h	93	100
8	Cu(II)-TD@nSiO_2[e] (0.3 mol%)	rt/sodium ascorbate, H_2O/EtOH (2 : 1)	20 min	99	101
9	SiO_2–NHC[h]-Cu(I)[f] (1 mol%)	80 °C/H_2O	6 h	98	102
10	PS-C22-CuI[g] (0.6 mol%)	Rt/H_2O	15 h	99	61
11	CuNPs/Mag silica (4.3 mol%)	70 °C/H_2O	1 h	98	103
12	MNP@PILCu[h] (4 mg)	50 °C/H_2O	2.5 h	95	104
13	MNP@PDMA-Cu[i] (0.3 mol%)	50 °C/H_2O, sodium ascorbate	2 h	96	74
14	Cu@βCD-PEG-mesoGO[j] (5 mol%)	25 °C/H_2O	1 h	90	105
15	Cu(II)/NP (0.06 g)	rt/MeOH	1 min	99	This study

[a] Reaction condition: three-component reaction of the benzyl bromide, phenyl acetylene and NaN_3. [b] Porphyrin-bridged silsesquioxane (PBS). [c] Copper nanoparticles on activated carbon (CuNP/C). [d] Nano-copper (CuNP). [e] Copper Immobilized on Nano silica Triazine Dendrimer. [f] N-heterocyclic carbene. [g] Polystyrene resin-supported copper(I) iodide-cryptand-22 complex. [h] Magnetic nanoparticles into the cross-linked poly(imidazole/imidazolium) immobilized Cu(II). [i] Copper sulphate onto multi-layered poly (2-dimethylaminoethyl acrylamide)-coated Fe_3O_4 nanoparticles. [j] Copper supported β-cyclodextrin functionalized PEGylated mesoporous silica nanoparticle-graphene oxide hybrid.

more time (Table 8, entry 6). Although, the reactions by using Cu(II)-TD@nSiO_2 and PS-C22-Cu(I) complexes as catalysts are completed at room temperature but they suffer from hard and lengthy preparation process (Table 8, entries 8 and 10). Although the syntheses in the presence of some catalysts, like 2-pyrrole carbaldiminato-Cu(II) complex, Cu(I)-zeolite, Cu NP and PS-C22-CuI, were carried out at room temperature, they took much longer reaction times (Table 8, entries 1,3,7 and 10). The preparations of CuNPs/Mag Silica, MNP@PILCu, MNP@PDMA-Cu and Cu@βCD-PEG-mesoGO are also difficult or costly (Table 8, entries 11–14). The advantages of Cu(II)/NP as catalyst for the synthesis of 1,4-disubstituted-1,2,3-triazole **8a** are listed in Table 8, entry 15.

Conclusions

In summary, we established copper nitrate, supported on mesopores of natural phosphate (Cu(II)/NP), as new, inexpensive, eco-friendly and recyclable heterogeneous catalyst for the synthesis of heteroatom-containing chemicals including xanthene and 1,4-disubstituted-1,2,3-triazole in good to excellent yields. Cu(II)/NP efficiently catalyzed the synthesis of xanthenes by the condensation of aromatic aldehydes with 1,3-cyclic diketones in ethanol under the reflux condition. Cu(II)/NP also showed as an efficient catalyzer in the regioselective synthesis of 1,4-disubstituted-1,2,3-triazoles *via* azide/alkyne ''click''-reaction or CuAAC reaction at room temperature. The reaction for the

synthesis of 1,4-disubstituted-1,2,3-triazoles proceeded by using stable Cu(II) instead of unstable Cu(I) species in the absence of any ligand or base. By using the heterogeneous catalyst Cu(II)/NP, the processes afforded the products with high yields in short reaction times, while the preparation process of the catalyst was easy, using inexpensive materials, recyclable, environmentally benign, stable, and almost leaching-free. The use of natural phosphate (NP) as a support for Cu(II) provides the advantages due to its excellent stability (both chemical and thermal), high surface area, low cost, and availability.

Conflicts of interest

There are no conflicts of interest to declare.

Acknowledgements

We are grateful of Payame Noor University (PNU) for their partial support, Mazandaran University of Medical Sciences for providing laboratory facilities to carry out this research and Australian College of Kuwait for the funding of IRC-2017-18-SOE-ME-PR01 and PR02 is also acknowledged.

Notes and references

1 M. J. Hülsey, H. Yang and N. Yan, *ACS Sustainable Chem. Eng.*, 2018, **6**, 5694–5707.
2 X. Chen, H. Yang, M. J. Hülsey and N. Yan, *ACS Sustainable Chem. Eng.*, 2017, **5**, 11096–11104.
3 S. Rostamnia and E. Doustkhah, *RSC Adv.*, 2014, **4**, 28238–28248.
4 F. Rajabi, M. Pinilla-de Dios and R. Luque, *Catalysts*, 2017, **7**, 216.
5 F. Bazi, H. El Badaoui, S. Tamani, S. Sokori, L. Oubella, M. Hamza, S. Boulaajaj and S. Sebti, *J. Mol. Catal. A: Chem.*, 2006, **256**, 43–47.
6 M. Zhang, Y. Zhao, Q. Liu, L. Yang, G. Fan and F. Li, *Dalton Trans.*, 2016, **45**, 1093–1102.
7 A. Chen and P. Holt-Hindle, *Chem. Rev.*, 2010, **110**, 3767–3804.
8 D. Kim, C. S. Kley, Y. Li and P. Yang, *Proc. Natl. Acad. Sci. U. S. A.*, 2017, **114**, 10560–10565.
9 R. van den Berg, G. Prieto, G. Korpershoek, L. I. van der Wal, A. J. van Bunningen, S. Lægsgaard-Jørgensen, P. E. de Jongh and K. P. de Jong, *Nat. Commun.*, 2016, **7**, 13057.
10 B. S. Anandakumar, M. B. M. Reddy, C. N. Tharamani, M. A. Pasha and G. T. Chandrappa, *Chin. J. Catal.*, 2013, **34**, 704–710.
11 M. Domínguez, F. Romero-Sarria, M. Centeno and J. Odriozola, *Appl. Catal., B*, 2009, **87**, 245–251.
12 Z. Weng, Y. Wu, M. Wang, J. Jiang, K. Yang, S. Huo, X.-F. Wang, Q. Ma, G. W. Brudvig, V. S. Batista, Y. Liang, Z. Feng and H. Wang, *Nat. Commun.*, 2018, **9**, 415.
13 T. Yasukawa, A. Suzuki, H. Miyamura, K. Nishino and S. Kobayashi, *J. Am. Chem. Soc.*, 2015, **137**, 6616–6623.
14 J. Jia, C. Qian, Y. Dong, Y. F. Li, H. Wang, M. Ghoussoub, K. T. Butler, A. Walsh and G. A. Ozin, *Chem. Soc. Rev.*, 2017, **46**, 4631–4644.
15 A. Smahi, A. Solhy, R. Tahir, S. Sebti, J. A. Mayoral, J. I. García, J. M. Fraile and M. Zahouily, *Catal. Commun.*, 2008, **9**, 2503–2508.
16 S. d. Sebti, A. Solhy, R. Tahir, S. Abdelatif, S. d. Boulaajaj, J. A. Mayoral, J. I. García, J. M. Fraile, A. Kossir and H. Oumimoun, *J. Catal.*, 2003, **213**, 1–6.
17 Q. Y. Ma, T. J. Logan and S. J. Traina, *Environ. Sci. Technol.*, 1995, **29**, 1118–1126.
18 A. Aklil, M. Mouflih and S. Sebti, *J. Hazard. Mater.*, 2004, **112**, 183–190.
19 M. Vila, S. Sánchez-Salcedo, M. Cicuéndez, I. Izquierdo-Barba and M. Vallet-Regí, *J. Hazard. Mater.*, 2011, **192**, 71–77.
20 X. Cao, L. Q. Ma, D. R. Rhue and C. S. Appel, *Environ. Pollut.*, 2004, **131**, 435–444.
21 M. Šljivić, I. Smičiklas, I. Plećaš and M. Mitrić, *Chem. Eng. J.*, 2009, **148**, 80–88.
22 E. Vieira, J. Huwyler, S. Jolidon, F. Knoflach, V. Mutel and J. Wichmann, *Bioorg. Med. Chem. Lett.*, 2005, **15**, 4628–4631.
23 H. Hafez, M. Hegab, I. Ahmed-Farag and A. El-Gazzar, *Bioorg. Med. Chem. Lett.*, 2008, **18**, 4538–4543.
24 Y. Kitahara and K. Tanaka, *Chem. Commun.*, 2002, 932–933.
25 B. Maleki, A. Davoodi, M. V. Azghandi, M. Baghayeri, E. Akbarzadeh, H. Veisi, S. S. Ashrafi and M. Raei, *New J. Chem.*, 2016, **40**, 1278–1286.
26 C. G. Knight and T. Stephens, *Biochem. J.*, 1989, **258**, 683–687.
27 M. Ahmad, T. A. King, D.-K. Ko, B. H. Cha and J. Lee, *J. Phys. D: Appl. Phys.*, 2002, **35**, 1473.
28 B. Karami, K. Esk and G. Ansari, *Chem. Sin.*, 2017, **8**, 342–354.
29 F. N. Sadeh, M. Fatahpour, N. Hazeri, M. T. Maghsoodlou and M. Lashkari, *Acta Chem. Iasi*, 2017, **25**, 24–37.
30 S. Rezayati, H. Seifournia and E. Mirzajanzadeh, *Asian J. Green Chem.*, 2017, **1**, 24–33.
31 A. Khazaei, M. Rezaei, A. R. Moosavi-Zare and S. Saednia, *J. Chin. Biochem. Soc.*, 2017, **64**, 1088–1095.
32 F. S. Arbosara, F. Shirini, M. Abedini and H. F. Moafi, *J. Nanostruct. Chem.*, 2015, **5**, 55–63.
33 A. Javid, M. M. Heravi and F. F. Bamoharram, *J. Chem.*, 2011, **8**, 910–916.
34 P. Sivaguru and A. Lalitha, *Chin. Chem. Lett.*, 2014, **25**, 321–323.
35 M. Esmaeilpour, J. Javidi, F. Dehghani and F. Nowroozi Dodeji, *New J. Chem.*, 2014, **38**, 5453–5461.
36 R. N. Baig and R. S. Varma, *Green Chem.*, 2012, **14**, 625–632.
37 L. Kashmiri and Y. Pinki, *Anti-Cancer Agents Med. Chem.*, 2018, **18**, 21–37.
38 B. Wang, B. Zhao, Z.-S. Chen, L.-P. Pang, Y.-D. Zhao, Q. Guo, X.-H. Zhang, Y. Liu, G.-Y. Liu, Z. Hao, X.-Y. Zhang, L.-Y. Ma and H.-M. Liu, *Eur. J. Med. Chem.*, 2018, **143**, 1535–1542.
39 I. Mohammed, I. R. Kummetha, G. Singh, N. Sharova, G. Lichinchi, J. Dang, M. Stevenson and T. M. Rana, *J. Med. Chem.*, 2016, **59**, 7677–7682.

40 C. Wu, B. Eck, S. Zhang, J. Zhu, A. D. Tiwari, Y. Zhang, Y. Zhu, J. Zhang, B. Wang, X. Wang, X. Wang, J. You, J. Wang, Y. Guan, X. Liu, X. Yu, B. D. Trapp, R. Miller, J. Silver, D. Wilson and Y. Wang, *J. Med. Chem.*, 2017, **60**, 987–999.
41 D. Dheer, V. Singh and R. Shankar, *Medicinal Attributes of 1,2,3-Triazoles*, Current Developments, 2017.
42 A. Espinoza-Vazquez, F. J. Rodriguez-Gomez, B. I. Vergara-Arenas, L. Lomas-Romero, D. Angeles-Beltran, G. E. Negron-Silva and J. A. Morales-Serna, *RSC Adv.*, 2017, **7**, 24736–24746.
43 N. P. Debia, M. T. Saraiva, B. S. Martins, R. Beal, P. F. B. Gonçalves, F. S. Rodembusch, D. Alves and D. S. Lüdtke, *J. Org. Chem.*, 2018, **83**, 1348–1357.
44 K. D. Gavlik, E. S. Sukhorukova, Y. M. Shafran, P. A. Slepukhin, E. Benassi and N. P. Belskaya, *Dyes Pigm.*, 2017, **136**, 229–242.
45 F. Alonso, Y. Moglie, G. Radivoy and M. Yus, *Adv. Synth. Catal.*, 2010, **352**, 3208–3214.
46 C. W. Tornøe, C. Christensen and M. Meldal, *J. Org. Chem.*, 2002, **67**, 3057–3064.
47 M. S. Singh, S. Chowdhury and S. Koley, *Tetrahedron*, 2016, **72**, 5257–5283.
48 M. Meldal and C. W. Tornøe, *Chem. Rev.*, 2008, **108**, 2952–3015.
49 V. O. Rodionov, S. I. Presolski, S. Gardinier, Y.-H. Lim and M. Finn, *J. Am. Chem. Soc.*, 2007, **129**, 12696–12704.
50 F. Himo, T. Lovell, R. Hilgraf, V. V. Rostovtsev, L. Noodleman, K. B. Sharpless and V. V. Fokin, *J. Am. Chem. Soc.*, 2005, **127**, 210–216.
51 S. Quader, S. E. Boyd, I. D. Jenkins and T. A. Houston, *J. Org. Chem.*, 2007, **72**, 1962–1979.
52 A. Sarkar, T. Mukherjee and S. Kapoor, *J. Phys. Chem. C*, 2008, **112**, 3334–3340.
53 S. Chassaing, M. Kumarraja, A. Sani Souna Sido, P. Pale and J. Sommer, *Org. Lett.*, 2007, **9**, 883–886.
54 I. Jlalia, H. Elamari, F. Meganem, J. Herscovici and C. Girard, *Tetrahedron Lett.*, 2008, **49**, 6756–6758.
55 T. Miao and L. Wang, *Synthesis*, 2008, **2008**, 363–368.
56 B. H. Lipshutz and B. R. Taft, *Angew. Chem., Int. Ed.*, 2006, **45**, 8235–8238.
57 M. L. Kantam, V. S. Jaya, B. Sreedhar, M. M. Rao and B. M. Choudary, *J. Mol. Catal. A: Chem.*, 2006, **256**, 273–277.
58 K. Yamaguchi, T. Oishi, T. Katayama and N. Mizuno, *Chem.–Eur. J.*, 2009, **15**, 10464–10472.
59 G. Molteni, C. L. Bianchi, G. Marinoni, N. Santo and A. Ponti, *New J. Chem.*, 2006, **30**, 1137–1139.
60 D. Wang, N. Li, M. Zhao, W. Shi, C. Ma and B. Chen, *Green Chem.*, 2010, **12**, 2120–2123.
61 B. Movassagh and N. Rezaei, *Tetrahedron*, 2014, **70**, 8885–8892.
62 K. Lal and P. Rani, *ARKIVOC*, 2016, **i**, 307–341.
63 C. Zhou, J. Zhang, P. Liu, J. Xie and B. Dai, *RSC Adv.*, 2015, **5**, 6661–6665.
64 J. M. Fraile, J. I. García, J. A. Mayoral, S. Sebti and R. Tahir, *Green Chem.*, 2001, **3**, 271–274.
65 S. Kantevari, R. Bantu and L. Nagarapu, *J. Mol. Catal. A: Chem.*, 2007, **269**, 53–57.
66 V. Thanikachalam, A. Arunpandiyan, J. Jayabharathi, C. Karunakaran and P. Ramanathan, *RSC Adv.*, 2014, **4**, 62144–62152.
67 C. W. Tornøe, C. Christensen and M. Meldal, *J. Org. Chem.*, 2002, **67**, 3057–3064.
68 J. C. Elliott, *Structure and chemistry of the apatites and other calcium orthophosphates*, Elsevier, 2013.
69 H. R. Ramananarivo, A. Solhy, J. Sebti, A. Smahi, M. Zahouily, J. Clark and S. Sebti, *ACS Sustainable Chem. Eng.*, 2013, **1**, 403–409.
70 A. Saber, A. Smahi, A. Solhy, R. Nazih, B. Elaabar, M. Maizi and S. d. Sebti, *J. Mol. Catal. A: Chem.*, 2003, **202**, 229–237.
71 S. Brunauer, L. S. Deming, W. E. Deming and E. Teller, *J. Am. Chem. Soc.*, 1940, **62**, 1723–1732.
72 A. J. Nathanael, D. Mangalaraj, S. Hong, Y. Masuda, Y. Rhee and H. Kim, *Mater. Chem. Phys.*, 2013, **137**, 967–976.
73 S. Kim, S. W. Kang, A. Kim, M. Yusuf, J. C. Park and K. H. Park, *RSC Adv.*, 2018, **8**, 6200–6205.
74 N. Zohreh, S. H. Hosseini, A. Pourjavadi and C. Bennett, *Appl. Organomet. Chem.*, 2016, **30**, 73–80.
75 M. Bagherzadeh, H. Mahmoudi, M. Amini, S. Gautam and K. H. Chae, *Sci. Iran.*, 2018, **25**, 1335–1343.
76 B. J. Borah, D. Dutta, P. P. Saikia, N. C. Barua and D. K. Dutta, *Green Chem.*, 2011, **13**, 3453–3460.
77 B. Małecka, A. Łącz, E. Drożdż and A. Małecki, *J. Therm. Anal. Calorim.*, 2015, **119**, 1053–1061.
78 A. Fallah, M. Tajbakhsh, H. Vahedi and A. Bekhradnia, *Res. Chem. Intermed.*, 2017, **43**, 29–43.
79 A. Małecki, R. Gajerski, S. Łabuś, B. Prochowska-Klisch and K. Wojciechowski, *J. Therm. Anal. Calorim.*, 2000, **60**, 17–23.
80 X. Gao, X. Chen, J. Zhang, W. Guo, F. Jin and N. Yan, *ACS Sustainable Chem. Eng.*, 2016, **4**, 3912–3920.
81 J. Albadi, M. Keshavarz, M. Abedini and M. Vafaie-Nezhad, *Chin. Chem. Lett.*, 2012, **23**, 797–800.
82 A. Corami, S. Mignardi and V. Ferrini, *Acta Geol. Sin. (Engl. Ed.)*, 2008, **82**, 1223–1228.
83 B. A. Dar, A. Bhowmik, A. Sharma, P. R. Sharma, A. Lazar, A. Singh, M. Sharma and B. Singh, *Appl. Clay Sci.*, 2013, **80**, 351–357.
84 J. Bennazha, M. Zahouily, S. Sebti, A. Boukhari and E. Holt, *Catal. Commun.*, 2001, **2**, 101–104.
85 J. C. Védrine, *Catalysts*, 2017, **7**, 341.
86 T. R. Mandlimath, B. Umamahesh and K. I. Sathiyanarayanan, *J. Mol. Catal. A: Chem.*, 2014, **391**, 198–207.
87 G. Song, B. Wang, H. Luo and L. Yang, *Catal. Commun.*, 2007, **8**, 673–676.
88 A. Pramanik and S. Bhar, *Catal. Commun.*, 2012, **20**, 17–24.
89 A. Khalafi-Nezhad, F. Panahi, S. Mohammadi and H. O. Foroughi, *J. Iran. Chem. Soc.*, 2013, **10**, 189–200.
90 A. John, P. J. P. Yadav and S. Palaniappan, *J. Mol. Catal. A: Chem.*, 2006, **248**, 121–125.
91 K. Niknam, F. Panahi, D. Saberi and M. Mohagheghnejad, *J. Heterocycl. Chem.*, 2010, **47**, 292.

92 T. R. Mandlimath, B. Umamahesh and K. I. Sathiyanarayanan, *J. Mol. Catal. A: Chem.*, 2014, **391**, 198–207.
93 M. Rahimifard, G. M. Ziarani, A. Badiei, S. Asadi and A. A. Soorki, *Res. Chem. Intermed.*, 2016, **42**, 3847–3861.
94 A. N. Dadhania, V. K. Patel and D. K. Raval, *J. Saudi Chem. Soc.*, 2017, **21**, S163–S169.
95 N. Mukherjee, S. Ahammed, S. Bhadra and B. C. Ranu, *Green Chem.*, 2013, **15**, 389–397.
96 V. Bénéteau, A. Olmos, T. Boningari, J. Sommer and P. Pale, *Tetrahedron Lett.*, 2010, **51**, 3673–3677.
97 C. S. Radatz, L. d. A. Soares, E. R. Vieira, D. Alves, D. Russowsky and P. H. Schneider, *New J. Chem.*, 2014, **38**, 1410–1417.
98 A. N. Prasad, B. M. Reddy, E.-Y. Jeong and S.-E. Park, *RSC Adv.*, 2014, **4**, 29772–29781.
99 F. Alonso, Y. Moglie, G. Radivoy and M. Yus, *Org. Biomol. Chem.*, 2011, **9**, 6385–6395.
100 L. Huang, W. Liu, J. Wu, Y. Fu, K. Wang, C. Huo and Z. Du, *Tetrahedron Lett.*, 2014, **55**, 2312–2316.
101 M. Nasr-Esfahani, I. Mohammadpoor-Baltork, A. R. Khosropour, M. Moghadam, V. Mirkhani, S. Tangestaninejad and H. Amiri Rudbari, *J. Org. Chem.*, 2014, **79**, 1437–1443.
102 P. Li, L. Wang and Y. Zhang, *Tetrahedron*, 2008, **64**, 10825–10830.
103 F. Nador, M. A. Volpe, F. Alonso, A. Feldhoff, A. Kirschning and G. Radivoy, *Appl. Catal., A*, 2013, **455**, 39–45.
104 A. Pourjavadi, S. H. Hosseini, N. Zohreh and C. Bennett, *RSC Adv.*, 2014, **4**, 46418–46426.
105 S. Bahadorikhalili, L. Ma'mani, H. Mahdavi and A. Shafiee, *Microporous Mesoporous Mater.*, 2018, **262**, 207–216.